Commissioning of the adaptive optics supported LUCI instruments at the Large Binocular Telescope: results

Heidt, Jochen, Pramskiy, Alexander, Thompson, David, Seifert, Walter, Gredel, Roland, et al.

Jochen Heidt, Alexander Pramskiy, David Thompson, Walter Seifert, Roland Gredel, Doug Miller, Greg Taylor, Simone Esposito, Alfio Puglisi, Enrico Pinna, Andreas Quirrenbach, "Commissioning of the adaptive optics supported LUCI instruments at the Large Binocular Telescope: results," Proc. SPIE 10702, Ground-based and Airborne Instrumentation for Astronomy VII, 107020B (6 July 2018); doi: 10.1117/12.2313506

SPIE.

Event: SPIE Astronomical Telescopes + Instrumentation, 2018, Austin, Texas, United States

Commissioning of the adaptive optics supported LUCI instruments at the Large Binocular Telescope: results

Jochen Heidt[a], Alexander Pramskiy[a], David Thompson[b], Walter Seifert[a], Roland Gredel[c], Doug Miller[b], Greg Taylor[b], Simone Esposito[d], Alfio Puglisi[d], Enrico Pinna[d], and Andreas Quirrenbach[a]

[a]Landessternwarte, Zentrum für Astronomie der Universität Heidelberg, Königstuhl 12, 69117 Heidelberg, Germany
[b]LBT Observatory, University of Arizona, 933 N. Cherry Ave, Tucson, AZ 85721, USA
[c]Max-Planck Institut für Astronomie, Königstuhl 17, 69117 Heidelberg, Germany
[d]Arcetri Astrophysical Observatory, Largo E. Fermi 5, 50125 Firence, Italy

ABSTRACT

The LUCI instruments are a pair of NIR imagers and multi-object spectrographs located at the front bent Gregorian foci of the Large Binocular Telescope (LBT). One of their special features is their diffraction-limited imaging and long-slit spectroscopic capability in combination with the LBT adaptive secondary mirrors. This allows to achieve a spatial resolution down to 60mas and a spectral resolution of up to 25000. Switching from seeing-limited to diffraction-limited observations changes several operational aspects due to features such as the non-common path aberration or the flexure of the instruments. They all require novel techniques to optimize the image quality and to maximize the scientific return. Non-common path aberration can be corrected via look-up tables. For active flexure compensation the night-sky emission is used. The commissioning of the instruments in diffraction-limited mode on sky is largely finished and the instruments have been handed over to the LBT in April 2018.

Keywords: NIR instrumentation, adaptive optics observations, commissioning, active flexure compensation, Strehl ratio, Large Binocular Telescope

1. INTRODUCTION - THE LUCI INSTRUMENTS

The LUCI (formerly LUCIFER, Seifert et al., 2003[1]) instruments are fully-cryogenic near-infrared cameras and multi-object spectrographs at the Large Binocular Telescope (LBT) on Mt. Graham, Arizona. They have been developed by the Landessternwarte Heidelberg, the Max-Planck Institute for Extraterrestrial Physics, the Max-Planck Institute for Astronomy and the Astronomical Institute of the University of Bochum. LUCI1 and LUCI2 are installed at the SX and DX front bent-Gregorian focal stations of the LBT, respectively. Both instruments are identical in functionality and available observation modes. They have been in operation in seeing-limited mode since January 2010 (LUCI1) and September 2015 (LUCI2) and are being used in homogeneous binocular mode since 2017.

Imaging and spectroscopy is possible with the LUCI instruments using three cameras of different focal lengths. The two cameras for seeing-limited observations are refractive systems with f/1.8 and f/3.75 (N1.8 and N3.75 cameras), the diffraction limited camera is a modified two-mirror system with corrector, working at f/30 (N30-camera). The N3.75 imaging-camera projects a 4' × 4' FOV on the full 2k × 2k HAWAII2-RG detector, which results in a resolution of 0.12"/pixel (0.24" Nyquist). The N1.8 spectroscopy-camera images the 4' × 4' FOV on a quarter of the detector centered on the detector (0.25" resolution). It allows to record a full NIR band (z, J, H or K) spectrum for a slit centered in the FOV and the grating-tilt adjusted accordingly at R ∼ 2000-8000. Diffraction-limited imaging and spectroscopy is afforded by the N30 camera allowing for a usable FOV of 30" × 30" with 0.015"/pixel. With an 8.5 pixel (0.13") wide slit a spectral resolution of R ∼ 8000 - 25000 can be

Further author information: (Send correspondence to Jochen Heidt)
Jochen Heidt: E-mail: jheidt@lsw.uni-heidelberg.de, Telephone: +49 6221 541704

Ground-based and Airborne Instrumentation for Astronomy VII, edited by Christopher J. Evans, Luc Simard, Hideki Takami, Proc. of SPIE Vol. 10702, 107020B · © 2018 SPIE · CCC code: 0277-786X/18/$18 · doi: 10.1117/12.2313506

achieved. Imaging and spectroscopy can be performed with a wide range of up to 26 broad-band, medium-band, narrow-band and order sorting filters which are distributed in two filter wheels.

In spectroscopic mode, four gratings provide different resolution and wavelength coverage. A multi purpose grating (210 lines/mm) covers z, J, H and K-band spectroscopy at a resolution R $\sim$ 8000 for a 0.5" wide slit in seeing-limited mode and up to R $\sim$ 25000 with the 0.13" slit and the N30 camera. Depending on the camera, full-band spectra extend partly beyond the detector area. The second grating (200 lines/mm) acts as a low-resolution H+K grating at a resolution of R $\sim$ 2000 for a 0.5" slit. While this grating has been manufactured to deliver its best performance in H+K, it can be used as a z+J grating in 2nd order, too. The third grating (150 lines/mm) delivers a resolution of R $\sim$ 4000 at a high efficiency in Ks for a 0.5" slit. Finally, the fourth grating (40 lines/mm) is optimized for spectroscopy with adaptive optics (AO) and delivers a resolution of R $\sim$ 7000 in diffraction-limited mode with the 0.13" slit. At present, the gratings with 200 lines/mm and 210 line/mm are available in both LUCIs. The grating with 150 lines/mm is available in LUCI1 only, the grating with 40 lines/mm is available in LUCI2 only. Only the gratings with 40 lines/mm and with 210 lines/mm in LUCI2 have an optical quality to allow diffraction-limited spectroscopy. In principle, the grating with 40 lines/mm can also be used for seeing-limited spectroscopy at a very-low spectral resolution (R $\sim$ 900 for a 0.5" wide slit). It will even be possible to double-stack slits in the dispersion direction.

Spectroscopy can either be done in longslit or multi-object-slitmask (MOS) mode. For longslit observations, the unique MOS unit provides the instrument with 10 longslit, engineering and other masks which are permanently installed. In addition, 23 custom made exchangeable multi-slit masks can be stored and used in the instrument. The masks are laser-cut and are exchanged using auxiliary cryostats while preserving cryogenic conditions in the main instrument. These auxiliary cryostats temporarily attach to the main cryostat during the mask cabinet exchange. MOS spectroscopy is offered in seeing-limited mode only.

In the last four years, both LUCIs underwent substantial upgrades. Two new HAWAII-2RG detectors with a QE of about 80% over the entire zJHK-bands replaced the old HAWAII2 detectors. New optics and gratings allowed the start of the commissioning of the diffraction-limited mode of the LUCIs.

Progress obtained so far with the LUCI instruments has been reported by Mandel et al. (2006, 2008),[2,3] Ageorges et al. (2010),[4] Seifert et al. (2010),[5] and Buschkamp et al. (2012).[6] In this paper our results and experience with the diffraction-limited commissioning of LUCI1 and LUCI2 are presented. It started in January 2015 and was expected to be complete by the end of 2017. However, bad weather and technical issues resulted in a temporarily interruption of the commissioning. Thus, an "almost done" report is given.

The paper is organized as follows: In chapter 2, we describe the prerequisites for the start of the commissioning, which are the adaptive optics (AO) system as well as the hardware and software modifications necessary for the LUCI instruments. In chapter 3 we present the results of our commissioning with special emphasis on the non-common path aberration (NCPA), image quality, and the active flexure compensation (AFC) all of which are relevant for imaging and spectroscopy, respectively. Finally, we wrap up with a discussion of the open issues and an outlook.

2. PREREQUISITES FOR LUCI AO COMMISSIONING

2.1 The AO system

Both telescopes of the LBT are equipped with a high-order AO system called First Light Adaptive Optics (FLAO; Esposito et al. (2012)[7]). The FLAO system senses the atmospheric turbulence by means of a pyramid-based wavefront sensor, which samples the pupil on a grid of 30 $\times$ 30 subapertures. A corrected wavefront is obtained through an adaptive secondary mirror controlled by 672 actuators at a frequency of up to 1 kHz. On typical seeing values of 0.8", the FLAO provides, in the H band, high-order corrected images with Strehl ratios (SR) of about 80% on bright reference sources. A spatial resolution down to 60 mas can be achieved. For the correction a reference star down to 16th mag can be used, off-axis anywhere in a 2' $\times$ 3 FoV at reduced Strehl.

The system runs in 4 "binning-modes" for the wave-front sensor camera depending on the brightness of the reference star. These results in particular in the number of controlled modes used (400, 153, 66 and 36 for binning = 1-4, respectively; see Tab. 1 in Esposito et al. (2003)[7]). As the optical light feeding the FLAO system

and NIR light feeding the LUCIs has the same origin but is split by a dichroic, it is subject to NCPA. This needs to be corrected only in binnings 1 and 2, however.

2.2 LUCI hardware modifications

Newly developed diamond-turned metal mirror optics (AlSi42) for diffraction-limited observing were implemented in LUCI2 in autumn 2014 and newly developed Zerodur-based optics for diffracted-limited observing were installed in LUCI1 in summer 2015. At the same time two new gratings with 210 lines/mm and 40 lines/mm suitable for diffraction-limited spectroscopy were deployed in LUCI2. The Zerodur-based optics deliver a better image quality, yet the AO performance of LUCI1 and LUCI2 is similar as a dichroic splitting at 0.95 μm is used for LUCI2 and a dichroic splitting at 0.89 μm is used for LUCI1. This setup allows for z-band imaging and spectroscopy with LUCI1, but it reduces the light in the LUCI1 wave front sensor. For the AFC, new longslit and field stop masks for the N30 cameras with reference holes were manufactured.

2.3 LUCI software modifications

The LUCI software had to be extended considerably. Modifications include proper handling of two stars in the patrol field (one star for acquisition and collimation by the telescope, one reference star (RS) for wave-front sensing by the FLAO system), the development and implementation of a new code for AFC (see section 3.5.2 and Pramskiy et al. 2018, these proceedings), and an extension of the observation execution panel for use of the AFC by the observer. The positions of the two stars have to be specified by the observer via observing sequences. In addition, the observing tool (OT) which is offered by the LBT observatory (LBTO) to prepare the observing sequences had to be modified. AFC requires additional steps in an observing sequence to set up before science integrations can start, as compared to standard observations with passive flexure compensation (PFC).

3. AO COMMISSIONING - RESULTS

Basically all commissioning activities for the diffraction-limited modes took place between January 2015 and December 2017. To minimize the time required on sky, as much closed-dome testing as possible was carried out preceding on-sky runs. More than 100 sessions in closed dome were necessary to execute all tasks mostly for preparing the look-up tables for the NCPA, the PFC and development and fine-tuning of the parameters for the AFC. A substantial fraction of the tests were executed remotely from Italy or Germany. As it is very hard to get access to the telescope during daytime on working days due to competing teams or activities by LBTO, a substantial fraction of the work was done either during the periods of bad weather or during weekends.

On-sky commissioning was attempted during 12 commissioning runs in over 82 nights. Unfortunately, in only 37 nights we did have periods (or the full night) of "AO-weather", ie clear skies and DIMM seeing ≤ 1.2". At poorer seeing the FLAO system becomes unstable, thus the loop opens from time to time. In practice, LUCI AO-commissioning was carried out during 18 nights only. The remaining time on sky was mostly used for readiness tests of the FLAO systems, FLAO troubleshooting, and other tests by LBTO. A particular problem was to get the binning = 1 mode working stably over longer periods of time. The binning = 1 mode offers the highest correction and requires a RS < 10 mag.

Overall progress was hampered by various catastrophic incidents such as the glycol leak at one of the FLAO adaptive secondaries or LUCI MOS failures that resulted in the unavailability of one or two of the FLAO systems / LUCI instruments for almost a semester.

In spite of the various bottlenecks, the following milestones have been achieved:

- LUCI2 AO-imaging with short images and PFC has been offered in shared risk since spring 2017
- LUCI1 and LUCI2 AO-imaging with short images and PFC has been offered in binocular mode in shared risk since spring 2018
- LUCI1 and LUCI2 AO-imaging with AFC and PFC in binocular mode will be offered in shared risk starting autumn 2018

- Demonstration that AO-spectroscopy with AFC works on sky was achieved in December 2017.

In the following, the most important results of the diffraction-limited commissioning will be presented. Generally, if everything runs smoothly, there is only little difference between seeing-limited and diffraction-limited observing from an observer's point of view. The main difference is that for AO observing two stars (one for acquisition and collimation, one for wavefront sensing) must be specified. Also the overheads are a little bit higher. Typically, the Duty Cycle is $> 60\%$ for AO imaging with PFC and $> 70\%$ with AFC. The main reason for the difference is the much larger number of individual images/dithers for the same total integration time. While for broad-band imaging with PFC individual images are typically 1 min, they are about 5 min for narrow-band imaging with AFC. In spectroscopic mode with AFC, the Duty Cycle is similar to the the one for imaging with AFC.

3.1 Image scale, distortion and photometric zeropoints

The image scale for the N30-cameras as verified on accurate astrometry from globular clusters is 0.015"/pixel which is exactly within the specifications of 0.015"/pixel ± 20%. The distortion is very low, about 0.3% or 7 pixel (0.1") across the detector. A radial fit of the distortion gives $D(r) = 2.34284 \cdot 10^{-6} \cdot r^{1.8}$ for the N300 camera. The small distortion does not affect the acquisition of targets for the 8.5 pixel wide longslit as the target is normally close to the slit on the acquisition image.

In Tab. 1 the zero points for the N375 and N30 cameras are shown for both LUCI instruments. As expected, the photometric zero points for the two cameras are close to each other other between the cameras and the instruments. The only noticeable difference is in the z-filter (0.7 mag) which is due to the different cutoff wavelengths of the dichroics.

	zero point LUCI1		zero point LUCI2	
Filter	N3.75 [e^-/sec]	N30 [e^-/sec]	N30 [e^-/sec]	N3.75 [e^-/sec]
z	26.81±0.02	26.82±0.07	26.08±0.07	26.09±0.01
J	26.92±0.05	26.97±0.05	26.89±0.05	26.86±0.15
H	26.49±0.03	26.69±0.04	26.56±0.04	26.47±0.01
K	26.00±0.02	26.24±0.03	26.24±0.03	26.24±0.08
Ks	25.93±0.02	25.95±0.03	25.85±0.03	25.91±0.01

Table 1. Zero points in Vega-mag (e^-/sec) for the N3.75 and N30 cameras of the LUCI instruments. The gain is 2.0 e^-/ADU for both LUCI detectors.

3.2 Persistence, ghosts and crosstalk

Due to the sharp PSF on one hand and the nature of the HAWAII2-RG detectors on the other, persistence and channel crosstalk seriously affect the observations. In addition, since the bright reference star is very often on the detector itself, ghosts due to reflections make observations and data reduction more complicated. Fig. 1 shows examples of persistence, ghosts and channel crosstalk. By a clever design of the observations the impact can be minimized. For example, the jitter pattern in AO-spectroscopy should be chosen such that it avoids the position of the target during the acquisition. Alternatively, crossed filters leaving only a narrow wavelength range with $<<$ 1% peak efficiency may be used for the acquisition and alignment procedure. If the target is north of a bright star, position angles should be selected that avoid placing targets on the same column as saturated stars.

3.3 Non-common path aberration

Due to the NCPA, the shape of the PSF on the LUCI detector is significantly modified. Its correction is achieved by taking images with an artificial light source at 3-4 different elevations and covering the full rotator angle range. The procedure consists of applying a certain number to low order modes and identifying for each of this modes the best Zernicke coefficients in terms of achieved SR. The final signal generated by the full set of identified modes is saved as NCPA (also often called slope null vector) and used for observations on sky. In Fig. 2 the results of the NCPA determination with closed dome and the importance of correcting for it on sky are illustrated for LUCI1.

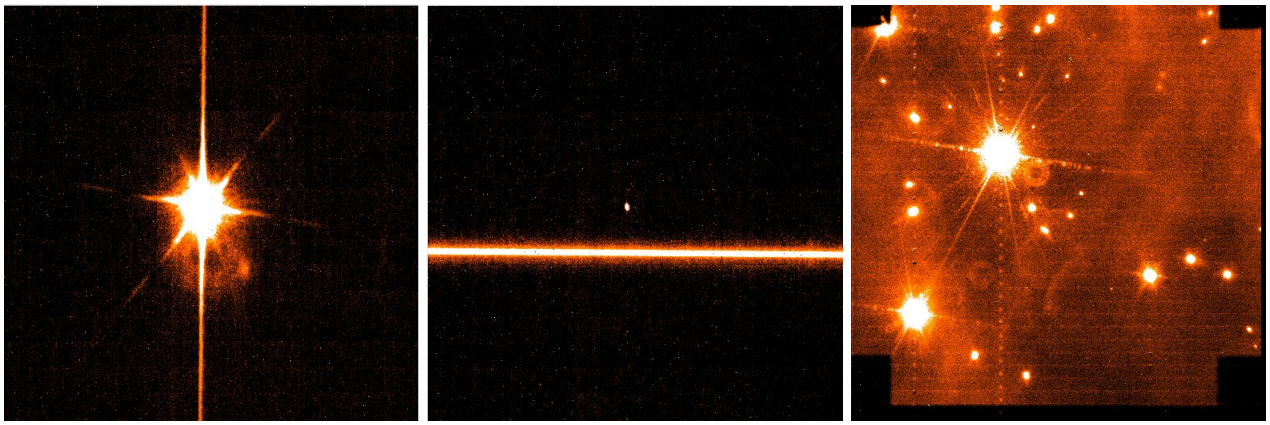

Figure 1. Left) Slit verification image after alignment of a bright star with the 0.13" longslit. Center) First spectrum after the alignment. The persistence from the bright star is the blob above the spectrum. It is $\leq 0.03\%$ of the input signal and fades with 1/t. In this case its peak intensity is almost 30% of the peak intensity of the spectrum. Right) Image with two bright stars. The ghost due the two brightest stars can easily be seen. Note the channel crosstalk pattern in y-direction along the two brightest stars.

3.4 Strehl ratio and image quality

During various occasions attempts were made to optimize the SR achievable. Fig. 3 shows the highest SR achieved so far on sky by observations of the R = H = 6.4 mag star HIP 15925 in H-band using an Fe II filter. The star itself was used as RS. During that night a SR of 75% was also achieved in the K-band (Brγ-filter) and 45% in the J-band (HeI-filter).

As already illustrated during the FLAO-commissioning, the SR achievable depends in the brightness of the reference star and the ambient seeing (see Fig. 2 in Esposito et al. (2003)[7]). On the other hand, this Figure also shows that the SR can vary widely even at the same ambient seeing. In addition, vibrations can plague the observations. We thus did not attempt to make our own diagram based on LUCI-FLAO observations.

During regular science observations extremely high SR (>> 60%) can be achieved, but hardly been measured. The LUCI instruments have neither a coronagraph nor neutral density filters. In addition, only full-frame readout is offered at present. With a minimum detector integration time (DIT) of 2.5 sec, even a 11th mag RS in binning = 2 is saturated. Windowed-observations, where the DIT could be considerably shorter, will not be offered.

RS covering the entire magnitude-range for AO-observations usable from m_R = 4 - 16 were successfully acquired during the commissioning. Point sources with underlying nebulosity (Sy I galaxies, stars with circumstellar discs) or binary stars with small (0.13") separation were successfully used for closing the loop. Problems occurred in dense stellar fields (globular clusters), where more than two stars were in the 2" FOV of the AO-lenslets used for correction by the FLAO systems. The loop was either not stable and/or different stars were selected by the SX/DX FLAO-systems for wave-front sensing resulting in a different image quality on both sides.

One of the most important aspects is the characterization of the image quality delivered by the FLAO+LUCI system as whole as function of the distance from the RS on the detector, as function of wavelength and to which amount stacking of images affect the apparent performance.

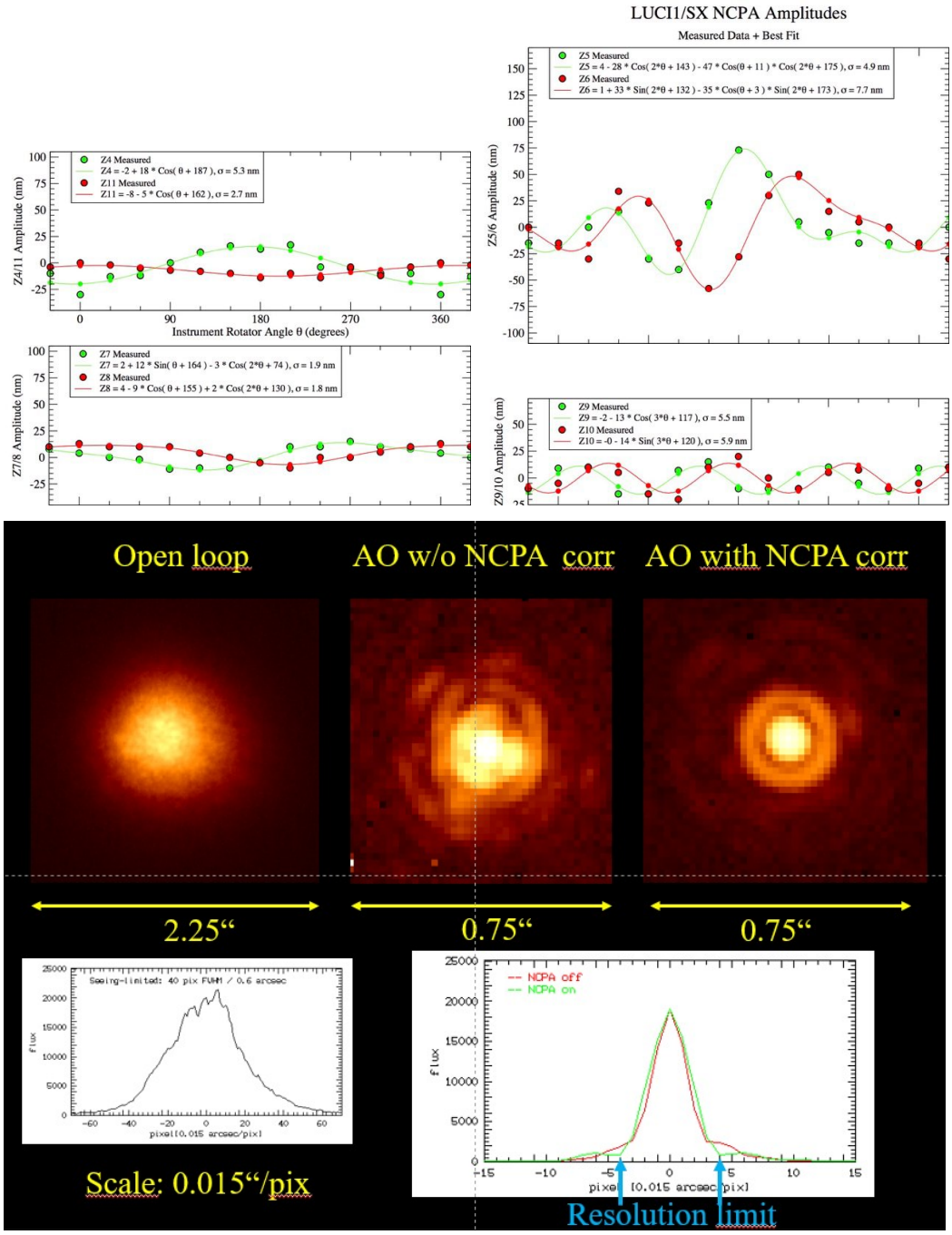

Figure 2. Top) NCPA determination for LUCI1. Bottom): Fe II image of a bright star with binning = 2 observed on-axis in open-loop (right) and closed-loop without (center) and with (right) NCPA correction. The difference is obvious. Below:) 1-dim cut through the centers of the AO-images above in x-direction. As can be seen, the NCPA correction is most important at about 4 pixels from the centers, which is at the resolution limit of the telescope. This may exactly be the region important eg for observations of extrasolar planets which are not doable otherwise.

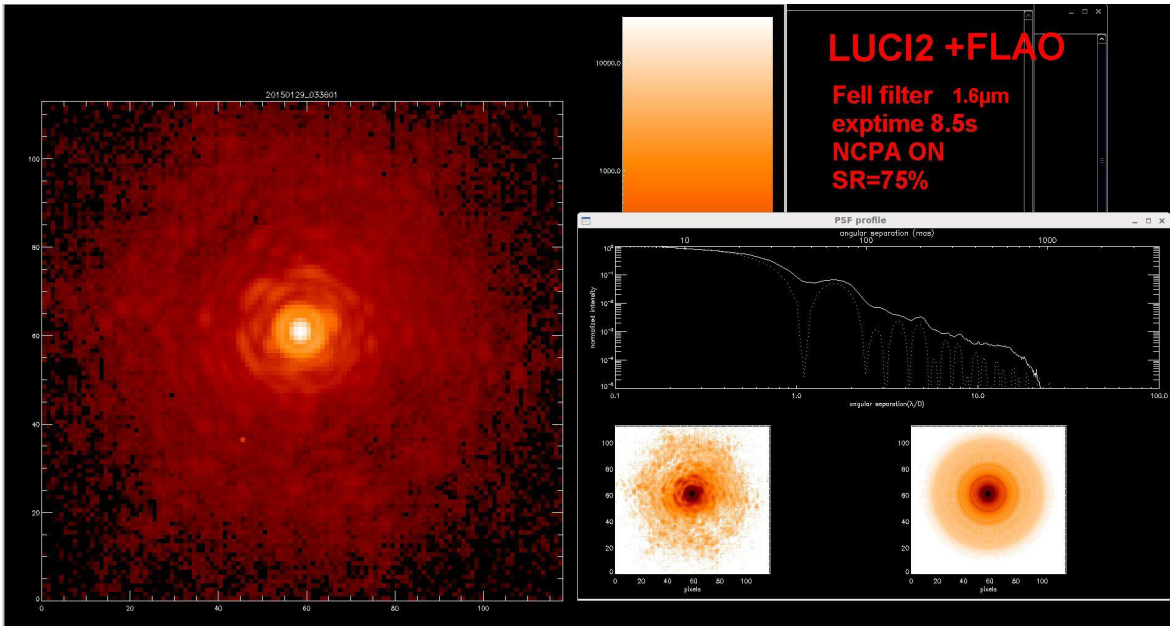

Figure 3. The highest SR achieved so far on sky with one of the LUCI instruments. Sub-window-readout 128 × 128 pixel, 0.15sec per DIT. Ambient DIMM seeing was 0.9".

Fig. 4 shows the SR as function or distance from the RS for about 1600 stars in the globular cluster M5. Compared are the results of a single image (1 min integration) versus a stacked (by integer pixel) image of 15 individual 1min integrations. The SR appears to be constant up to 8" radius and declines by about 15-20% across the full FOV. The SR of the stacks is lower by 9±2.5% on average compared to the single frames, which is due to PSF "smearing" due to integer shifts when combining images and possibly the much more heavier crowding on the combined image.

Fig. 5 shows the FWHM as derived from SExtractor for the same data set as above and J and K-band images of M5 taken in the same way. In addition, images taken at consecutively larger distances from the RS in H-band have also been analyzed. Obviously, the images are close to diffraction-limited in the inner few arcseconds around the RS. As expected the degradation of the image quality as a function of distance from the RS is wavelength dependent. Finally, even at distances of up to 1' of the RS, the image quality can be as good as 0.3" FWHM.

3.5 Flexure of the instrument and its correction

3.5.1 Passive flexure compensation

In seeing-limited mode, the flexure of the instrument is corrected internally via look-up tables, derived from the motion of an artificial light-source on the detector as function or rotator angle and elevation in closed-dome. The correction is done via one of the fold mirrors in the instrument for correction in x and y (or tip and tilt) which keeps the source on the detector on its position. The residual flexure is on the order of 0.5 pixel (0.12") during 30 min at $\delta = 0^{o}$ for the N1.8-camera used for spectroscopy. This is sufficient given the typical integration times for spectroscopy of 5min per position when nodding along the slit. For the N30-cameras this results in 8 pixel in 30min. This is not a problem for AO-supported broad-band imaging as even with the N30-camera images are photon noise dominated in 1min integrations. It becomes a problem, however, for AO-supported narrow-band imaging and/or spectroscopy as here much longer integrations of up to 20-30min per detector position are possible. The (spectroscopic) image quality will be degraded considerably resulting also in the loss of spectral resolution. Thus PFC is not sufficient for AO narrow-band imaging and long-slit spectroscopy.

3.5.2 Active flexure compensation

To solve the problem described in the previous section, the concept of the AFC was developed, tested and implemented throughout the entire commissioning period. A full description of this novel method can be found in Pramskiy et al. (2018, these proceedings). Thus we will here summarize only the most important details.

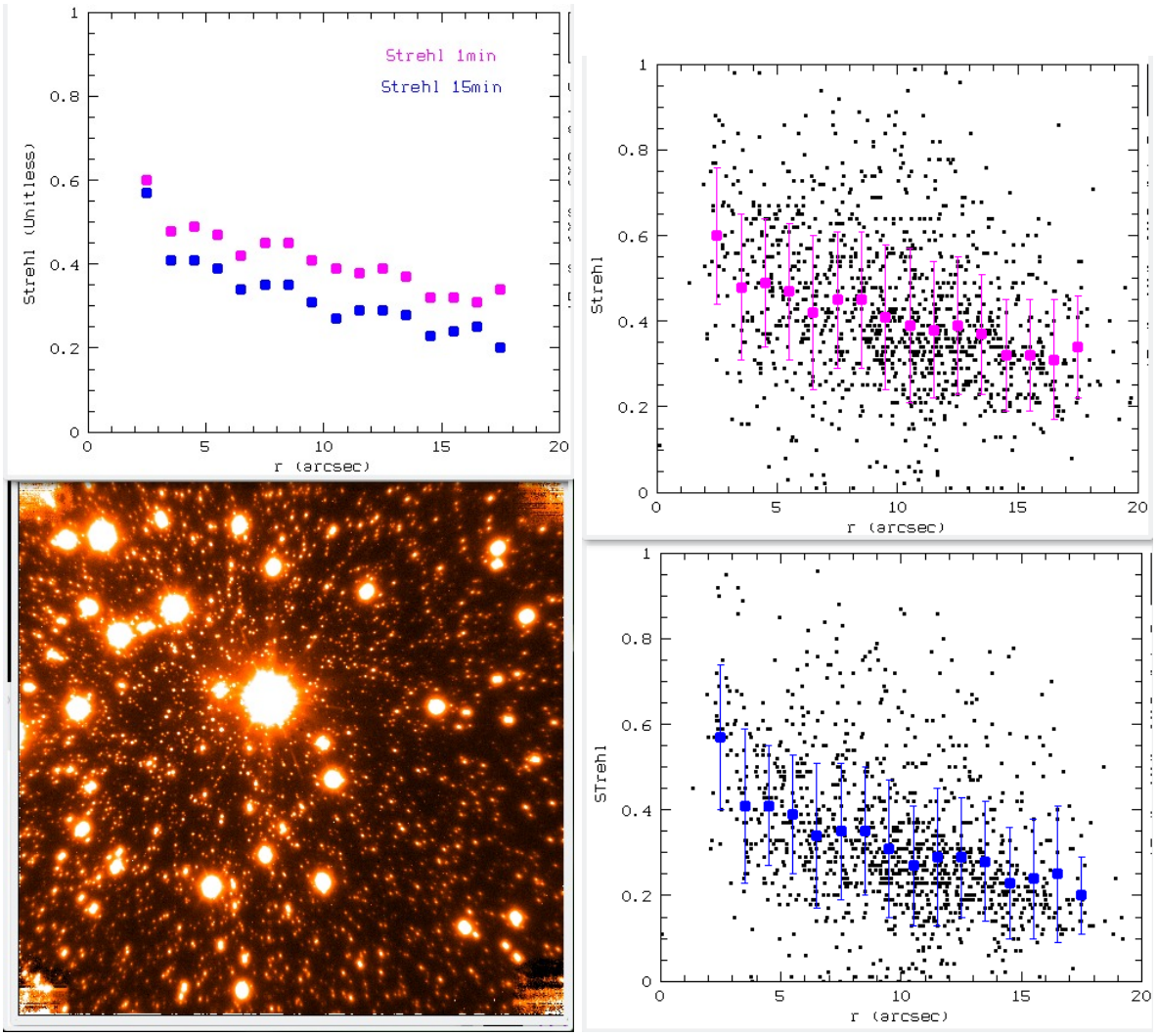

Figure 4. SR as a function of distance from the reference star (the brightest star in the 30" × 30" image in the lower left) for a 1min image (top right) and the 15min image (bottom right). Individual stars are plotted as black dots, cyan/blue symbols give median and std deviation around mean. The SR averages are directly compared in the figure on top left.

The working principle of the AFC is simple. Each mask used for AFC during the observations (either the field stop masks for imaging or the 0.13" long-slit mask for spectroscopy) contains a set of pinholes. The pinholes are either illuminated by the integrated night-sky (imaging) or are used as "slits" to take spectra of the night-sky (spectroscopy). The flexure of the instrument to be corrected manifests itself as changes of the positions of the illuminated pinholes or the positions of the night-sky emission lines on the detector. The code takes advantage of the read-mode sample-up-the ramp (often abbreviated SRR mode), which allows non-destructive readouts during an integration. Each non-destructive readout is then used to determine the position of the integrated night-sky or night-sky emission lines with respect to a pre-defined position on the detector and a correction is applied via one of the fold mirrors within the LUCI instruments. For imaging and spectroscopy special masks were designed with a certain number of pinholes (4 × 10 for imaging and 2 × 53 for spectroscopy) in a special arrangement on the detector whose light is stacked to improve the S/N.

At present, there is one fundamental difference between the AFC startup procedures used for imaging and spectroscopy. In imaging mode, a short 10sec image is used to move the illuminated pinholes on the detector to pre-defined positions using one of the fold mirrors. Next, a short SRR image is taken, sub-window cutouts with predefined positions and boxes on the detector are extracted and stacked. The centroid of this stacked image

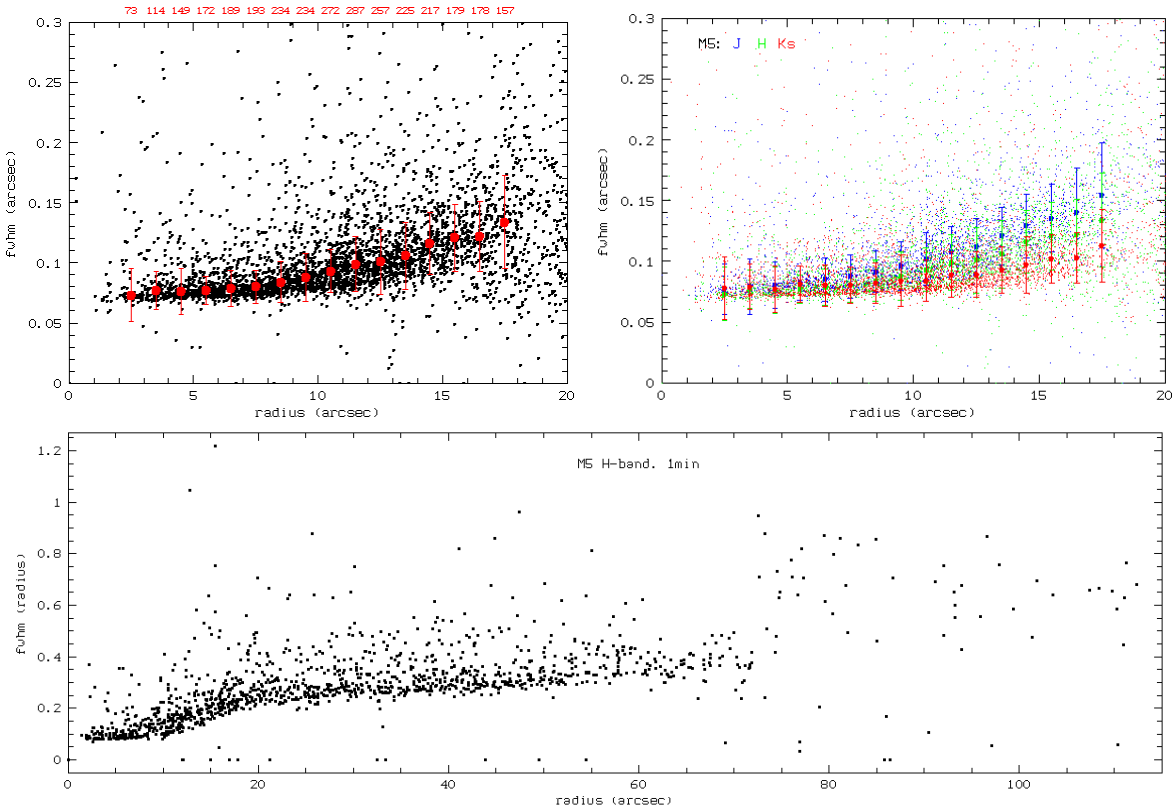

Figure 5. Top left) FWHM as a function of radius for about 2900 stars in the 30" × 30" FOV in M5. No brightness cut was applied, no deblending was attempted. Thus there is a substantial scatter towards larger FWHM. The red dots gives the median in bins of 1", the error bars the standard deviation of the mean. On top the number of stars per bin used is given. Top right) FWHM for JHKs-filters as function of distance from the RS. While there is basically no difference close to the RS, the degradation of image quality as function or wavelength becomes obvious at larger distances from the RS. Bottom) Image quality as a function of distance up to 2' from the RS.

is then used as reference. In spectroscopic mode a single frame is taken with the duration of the sampling time (time between two consecutive non-destructive reads in SRR-mode later in the AFC process, typically 30sec). This image is then copied multiple times according to the number of pinholes to be used and the images shifted depending on the relative positions of the pinholes with respect to each other. It turned out that the anamorphic magnification had considerable impact, so it is included in the software as well. These shifted images are then stacked and their centroid used as reference. The reason for this difference is the faintness of the night-sky emission lines, which cannot be seen in the individual pinholes and whose position is not known a priori with an accuracy of a few pixels. Once the AFC setup is complete, the sub-window cutouts with predefined positions and boxes on the detector based on the AFC setup are extracted, stacked and their deviation of the centroid with respect to the first one be used to correct for flexure via one of the fold mirrors in imaging and spectroscopic mode.

Extensive closed-dome test were carried out not only to optimize the method, but also to explore the brightness limits at which the AFC still works. At some point the S/N is too weak for the code to properly determine the centroid of the stacked night-sky image. Our current limit for the AFC to work is 0.04 counts/sec/pixel peak intensity. This implies that all broad- and narrow-band filters except two very narrow filters in the z-band can be used for AO imaging with AFC with typical intervals of 30 sec in SRR mode up to 85 deg elevation (where the gravity vector changes fast as a function of time). It is more critical for AO spectroscopy with AFC due to the low surface brightness of the night-sky emission lines with 0.015"/pixel. Due to the lack of on-sky time, we could only demonstrate that observations with AFC can be performed across the entire H-band and started with the K-band. We are confident that we may be able to demonstrate the use of the AFC in the K-band as

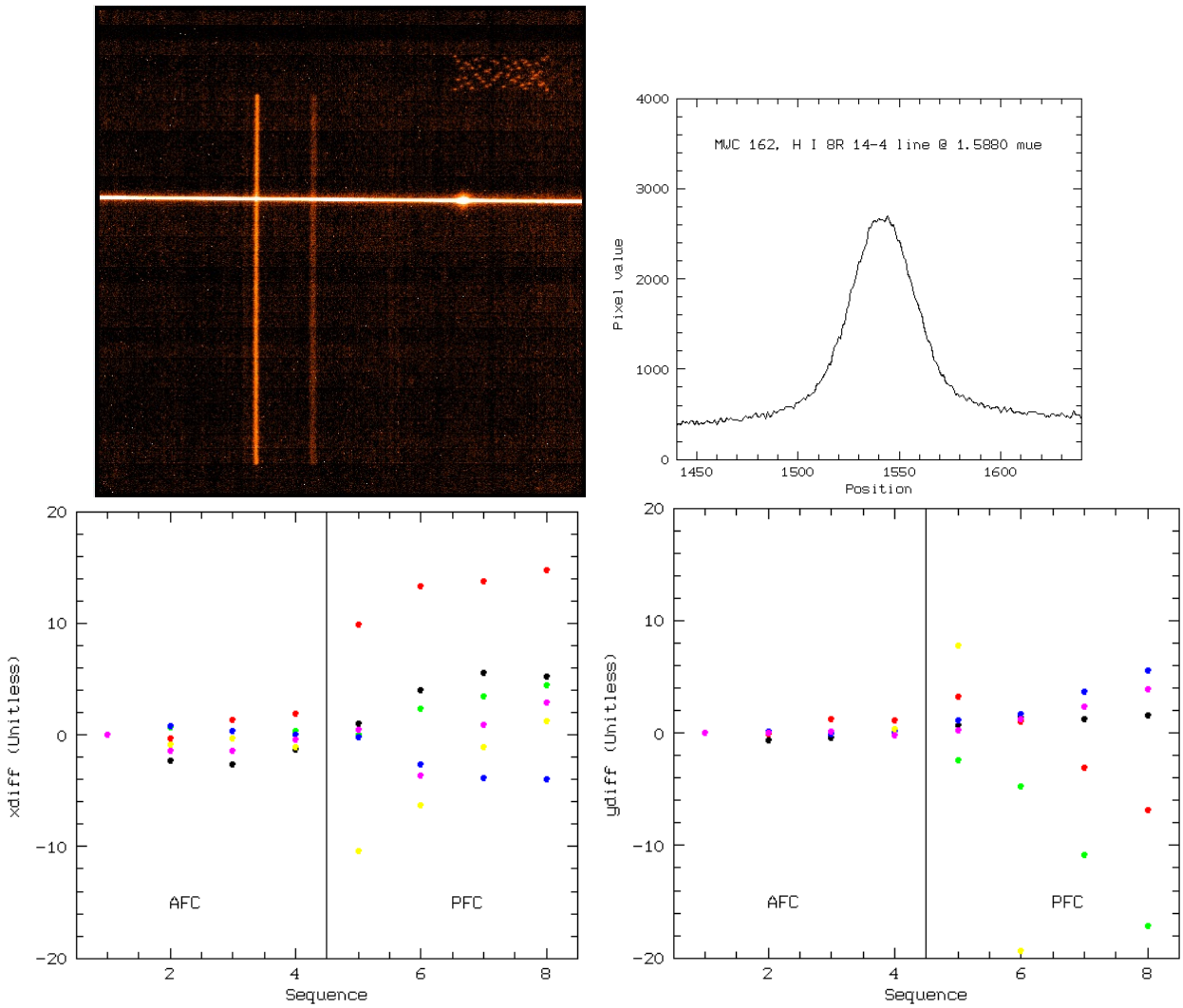

Figure 6. Top left) 2-dim spectrum of MWC 162 taken during AFC-tests. The wavelength range covered is 0.012 μm. The two night-sky emission lines from the longslit are at 1.5828 and 1.5843 μm, respectively. The Hydrogen recombination line from the target at 1.5880 μm can nicely be seen. The 1.5828 μm night-sky emission line through the AFC pinholes is located at the top right corner of the spectrum. The stack of these 53 emission lines is used for the AFC. The FWHM of the spectrum in spatial direction is 6.6 pixel (0.1"). Top right) 1-dim cut through the spectrum of MWC 162 at 1.5880 μm. The emission line has a FWHM of 37 pixel or $\sim$ 2.2 Å. Bottom) Comparison of the AFC and PFC for 6 measurements using 5 different night-sky emission lines in H- and K-band which have different intensities. For each series a star was aligned with the slit, the AFC started, followed by 4 integrations 5 min each. Then AFC was turned off and PFC on and another set of 4 integrations 5 min each was taken. Shown is the relative change of the position of the stacked and combined night-sky emission lines in x (left) and y (right) in pixel as a function of image number with respect to the first spectrum of a series of 8 spectra. The superior compensation via AFC over PFC is obvious. The improvement (ratio of the dispersion around the mean for AFC and PFC, respectively) is between 2 and 10. Note that this is already in a regime of mediocre S/N for our tests.

well, but we are sceptical for the J-band as the night-sky emission lines are much fainter in this band. However, our code allows to stack the signal of more than one night-sky line. This is particularly useful when observing with the grating with 40 lines/mm. This grating covers roughly one third of the NIR-bands per setup, which will allow to combine the emission from more than one bright line.

As expected from our closed-dome tests, the improvement on the correction for the flexure using AFC instead

of PFC can be as large as a factor of 10 - 20 depending on the S/N. This is illustrated in Fig. 6. The extra time required to set up the AFC during science observations is small, about 1-2min and has only little impact on the overall duty cycle.

We also tested the AFC in classical seeing-limited mode using just one pinhole. As one pixel in the N1.8-camera covers the sky area of 278 pixels in the N30-camera, S/N considerations are not an issue. As shown in Pramskiy et al. (2018, these proceedings) the AFC basically removes any shift of the night-sky emission lines from exposure to exposure thus improving the data quality considerably. We expect that the AFC will become standard for seeing-limited spectroscopy at the LBT in the near future.

3.6 Some additional results and comparison to other AO observations

In Fig. 8 we show a comparison of AO observations of the radio galaxy 3C 294 from KECKII und Subaru to our data. 3C 294 is about 10" east from a 10th mag star, which itself is a 0.155" separation binary star with an intensity ration 1:1.6 (see Fig. 7). Obviously, our image has a much better contrast although our exposure time was a factor of 5 shorter. 153 modes were corrected with a frequency of 625 Hz.

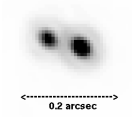

Figure 7. The RS star 10" east of 3C 294.

One of the most attractive applications of our system is the study of the circumstellar material of young stars. The stars itself can be used as RS having allowing for the the best correction in their environment. In Fig. 9 we show zJHKs-images of the Herbig Ae/Be star R Monocerotis, which has an extended circumstellar disk. The star is very red with R - K = 4.5 and shows strong wavelength-dependent changes of its structure in the innermost few arcseconds. Here only 66 modes were corrected with a frequency of 200 Hz.

In Fig. 10, finally, we show two extreme cases: a diffraction-limited image of a star just 2" off a 10.4 mag RS in the globular cluster M5 with 66mas FWHM and a 2 hour image of the gravitationally lensed z = 3.91 QSO APM 08279+5255. For the former 153 modes were corrected with a frequency of 625 Hz, while we could correct only for 36 modes at 100 Hz frequency for the latter. Although probably not spectacular, this image is impressive as a) the lensed QSO components were relatively faint for AO-work (the FLAO system gave an R-mag of 15.5), b) more than one component was used for the AO, c) the system was stable for about 3hrs during the 2 hour integration on target and d) it nevertheless produced images with 0.09" FWHM. Note that the 0.09" FWHM is only an *upper* limit as the three images of the QSO are lensed and are not necessarily point sources.

4. CURRENT STATUS, OPEN ISSUES AND OUTLOOK

The current status of the LUCI AO-commissioning can be described as follows:

- AO imaging imaging can be carried out with passive and with active flexure compensation in binocular mode.
- High resolution (R $\sim$ 20000) AO spectroscopy can be carried with LUCI2 and the grating with 210 lines/mm with *passive* flexure compensation. The availability is limited to bright stars and a relatively short period on target before image smearing and the loss of spectral resolution becomes problematic.
- High resolution (R $\sim$ 20000) AO spectroscopy can also be carried with LUCI2 and the grating with 210 lines/mm with *active* flexure compensation. However, this has been demonstrated only for the full H-band so far.

There are a two open issues, which need to be addressed before commissioning of the AO spectroscopy mode can resume. These are:

- Full control of the differential flexure between the FLAO systems and the LUCI instruments. Its does not impact AO imaging unless a star must be on the same location for a long period of time - a requirement for exoplanet transit observations - but AO spectroscopy, where a star needs to be centered on the slit on the same position on the detector for hours. The amplitude of the differential flexure can be as high as 0.25" during 2 hours at high ($> 80^o$) elevation which would led to a substantial degradation of the scientific output. At present tests are actively carried out to build look-up tables to correct for this effect. The aim is to reduce the amplitude of the differential flexure to about a tenth of the slit width.

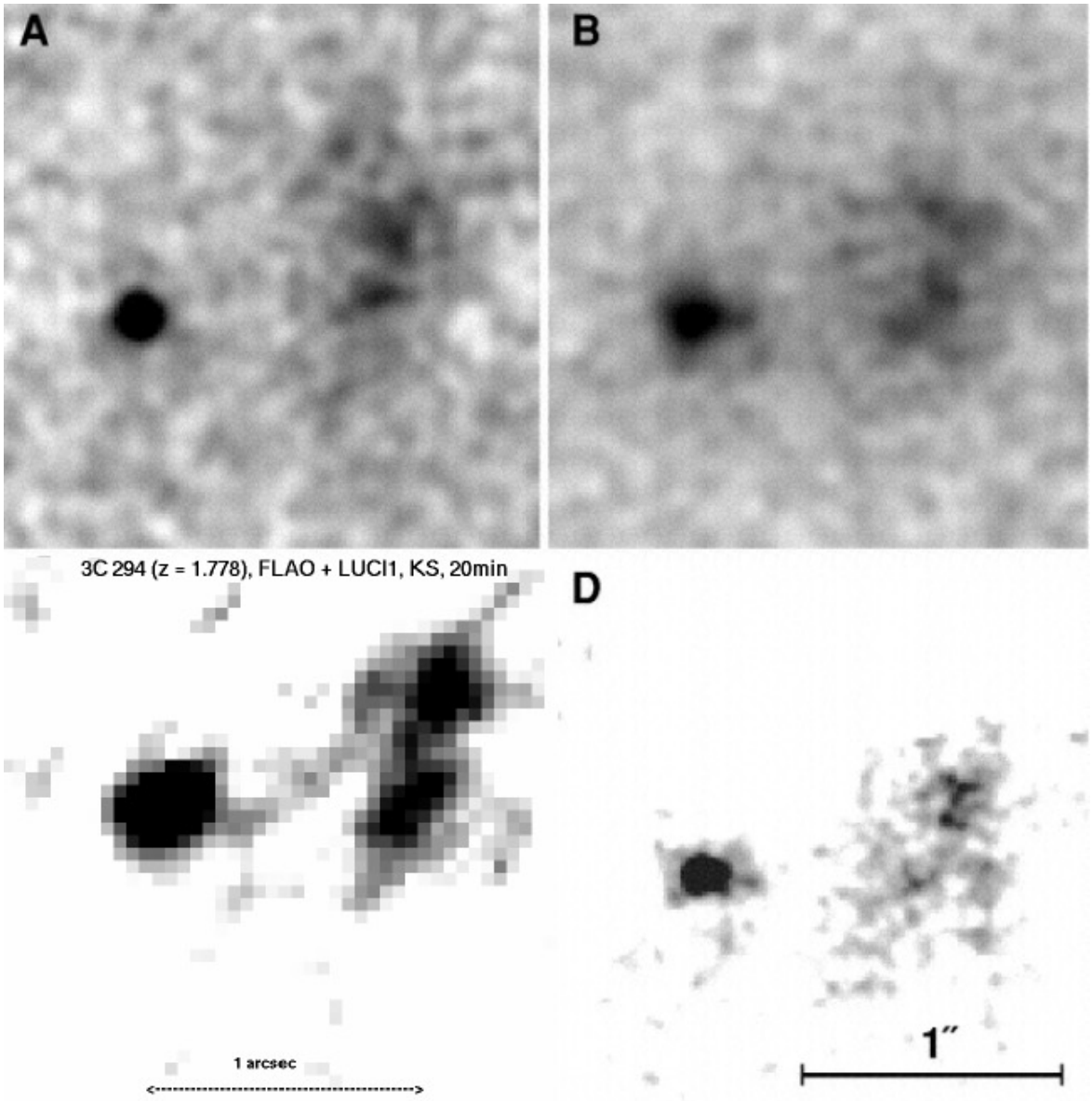

Figure 8. A) KECK II NIRSPEC AO K'-image (150 min) of 3C 294. B) Subaru IRCS AO K'-image (20 min). Both images are from Stockton et al. (2004).[8] D) KECK NIRSPEC AO H-image (100 min) from Quirrenbach et al. (2001).[9] Bottom left) Our own FLAO + LUCI1 Ks-image (20 min). The scale is the same in all images.

- We experience problems with the stability of the tilt of the grating with 40 lines/mm, the reason of which is currently under investigtion.

We hope that both of them are under control by summer 2018 and that LUCI2 AO-commissioning in spectrosopic mode can resume in fall 2018 with the aim to be done by the end of this year. Tests will include: a) proper correction of the differential flexure between the FLAO systems and the LUCI instruments, b) reliable functionality of the grating with 40 lines/mm; c) exploring the limits of the AFC supported AO-spectroscopy in the J and K-bands due to the faintness of the night-sky emission lines in these bands; and d) verification of the AFC in seeing-limited mode for multi-object spectroscopy. This should be achieved by a week long run.

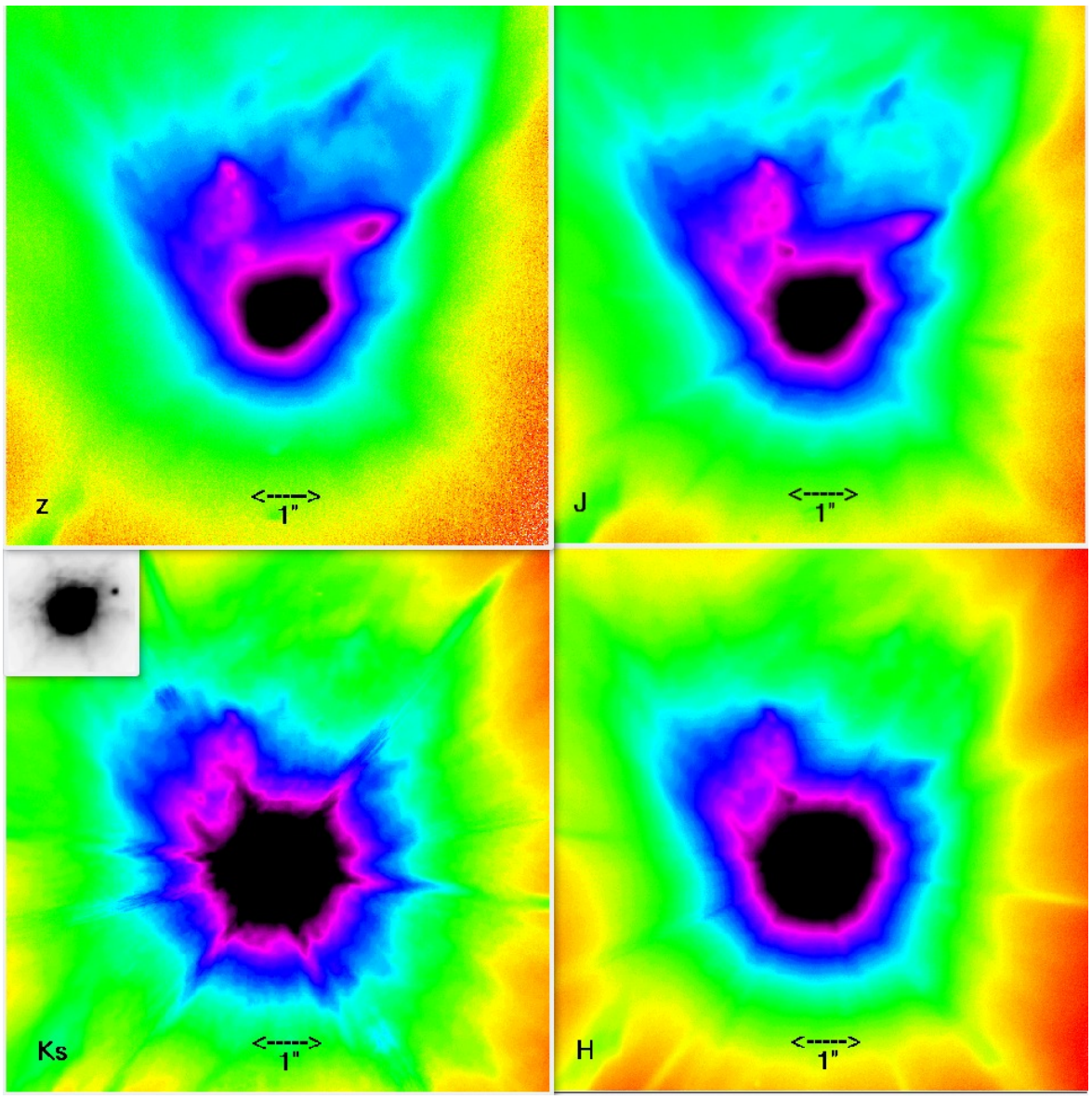

Figure 9. zJHKs-images of the Herbig Ae/Be star R Monocerotis. They are 8" on each side. Note the changes in the structure of the circumstellar disk on scales of tenths of arcseconds, in particular the disappearance of the arrow-like structure NW of the star with increasing wavelength. The star is a binary with 0.6" separation. It is shown as inlet in BW with a different dynamic range.

ACKNOWLEDGMENTS

This work was supported by the German federal department for education and research (BMBF) under the project numbers: 05 AL2VO1/8, 05 AL2EIB/4, 05 AL2EEA/1, 05 AL2PCA/5, 05 AL5VH1/5, 05 AL5PC1/1 and 05 A08VH1.

REFERENCES

[1] Seifert, W., Appenzeller, I., Baumeister, H., Bizenberger, P., Bomans, D., Dettmar, R.-J., Grimm, B., Herbst, T., Hofmann, R., Juette, M., Laun, W., Lehmitz, M., Lemke, R., Lenzen, R., Mandel, H., Polsterer, K., Rohloff, R.-R., Schuetze, A., Seltmann, A., Thatte, N. A., Weiser, P., and Xu, W., "LUCIFER: a

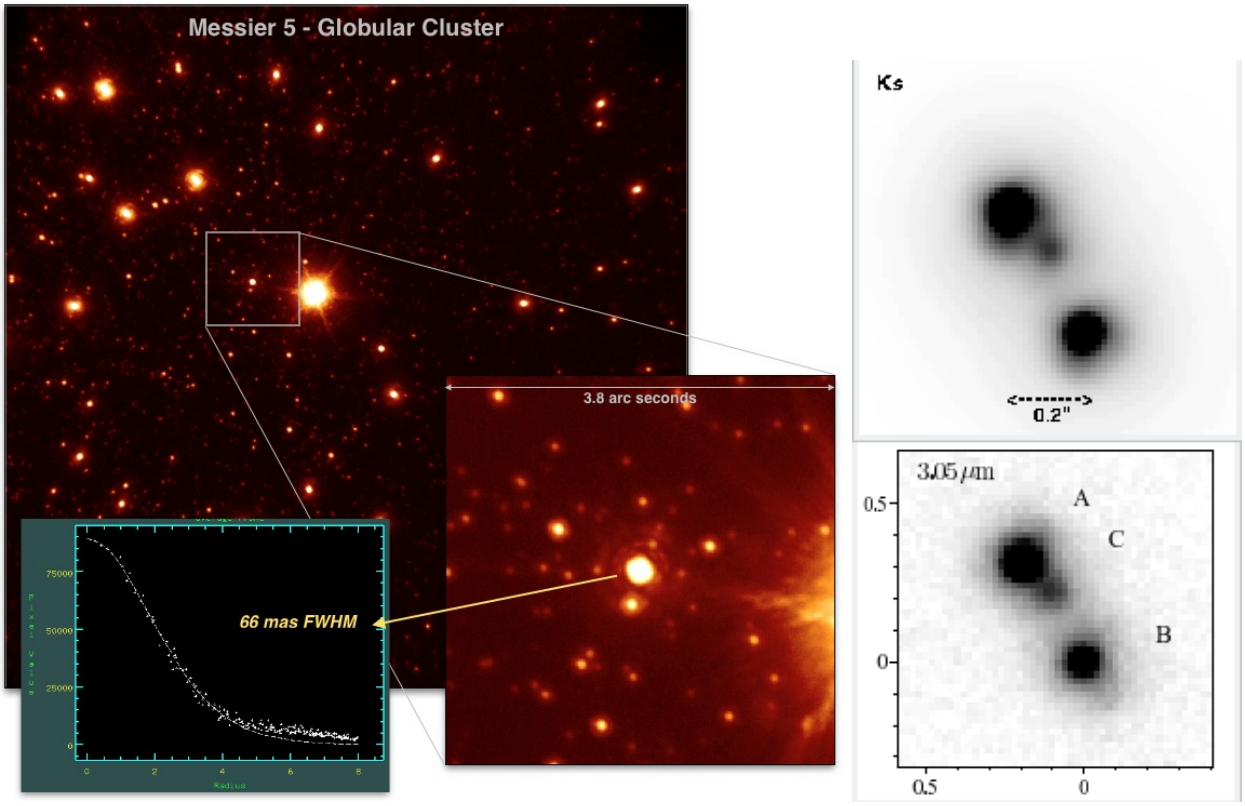

Figure 10. Left) Zoom into a star ~ 2" from the RS on H-band image of M5 showing a FWHM of 66mas. The image of this star is diffraction-limited. Right) Ks-band image (top) of the gravitationally lensed QSO APM 08279+5255 compared to a Subaru AO188 3.05 μm narrow-band image from Oya et al.(2013).[10] The separation of the components A and B is ~ 0.38" and the separation of the components A and C is ~ 0.14". The QSO itself (actually all components) was used as natural guide star, the FWHM of the individual components is ~ 0.09".

Multi-Mode NIR Instrument for the LBT," in [*Instrument Design and Performance for Optical/Infrared Ground-based Telescopes*], Iye, M. and Moorwood, A. F. M., eds., *Proc. SPIE* **4841**, 962–973 (2003).

[2] Mandel, H. G., Appenzeller, I., Seifert, W., Baumeister, H., Dettmar, R.-J., Feiz, C., Gemperlein, H., Germeroth, A., Grimm, B., Heidt, J., Herbst, T., Hofmann, R., Jütte, M., Knierim, V., Laun, W., Luks, T., Lehmitz, M., Lenzen, R., Polsterer, K., Quirrenbach, A., Rohloff, R.-R., Rosenberger, J., Weiser, P., and Weisz, H., "LUCIFER status report: Summer 2006," in [*Society of Photo-Optical Instrumentation Engineers (SPIE) Conference Series*], *Proc. SPIE* **6269**, 62693F (2006).

[3] Mandel, H., Seifert, W., Hofmann, R., Jütte, M., Lenzen, R., Ageorges, N., Bomans, D., Buschkamp, P., Dettmar, R.-J., Feiz, C., Gemperlein, H., Germeroth, A., Geuer, L., Heidt, J., Knierim, V., Laun, W., Lehmitz, M., Mall, U., Müller, P., Naranjo, V., Polsterer, K., Quirrenbach, A., Schäffner, L., Schwind, F., Weiser, P., and Weisz, H., "LUCIFER status report: summer 2008," in [*Ground-based and Airborne Instrumentation for Astronomy II*], *Proc. SPIE* **7014**, 70143S (2008).

[4] Ageorges, N., Seifert, W., Jütte, M., Knierim, V., Lehmitz, M., Germeroth, A., Buschkamp, P., Polsterer, K., Pasquali, A., Naranjo, V., Gemperlein, H., Hill, J., Feiz, C., Hofmann, R., Laun, W., Lederer, R., Lenzen, R., Mall, U., Mandel, H., Müller, P., Quirrenbach, A., Schäffner, L., Storz, C., and Weiser, P., "LUCIFER1 commissioning at the LBT," in [*Ground-based and Airborne Instrumentation for Astronomy III*], *Proc. SPIE* **7735**, 77351L (2010).

[5] Seifert, W., Ageorges, N., Lehmitz, M., Buschkamp, P., Knierim, V., Polsterer, K., Germeroth, A., Pasquali, A., Naranjo, V., Jütte, M., Feiz, C., Gemperlein, H., Hofmann, R., Laun, W., Lederer, R., Lenzen, R., Mall, U., Mandel, H., Müller, P., Quirrenbach, A., Schäffner, L., Storz, C., and Weiser, P., "LUCIFER1:

performance results," in [*Ground-based and Airborne Instrumentation for Astronomy III*], *Proc. SPIE* **7735**, 77357W (2010).

[6] Buschkamp, P., Seifert, W., Polsterer, K., Hofmann, R., Gemperlein, H., Lederer, R., Lehmitz, M., Naranjo, V., Ageorges, N., Kurk, J., Eisenhauer, F., Rabien, S., Honsberg, M., and Genzel, R., "LUCI in the sky: performance and lessons learned in the first two years of near-infrared multi-object spectroscopy at the LBT," in [*Ground-based and Airborne Instrumentation for Astronomy IV*], *Proc. SPIE* **8446**, 84465L (2012).

[7] Esposito, S., Riccardi, A., Pinna, E., Puglisi, A. T., Quirós-Pacheco, F., Arcidiacono, C., Xompero, M., Briguglio, R., Busoni, L., Fini, L., Argomedo, J., Gherardi, A., Agapito, G., Brusa, G., Miller, D. L., Guerra Ramon, J. C., Boutsia, K., and Stefanini, P., "Natural guide star adaptive optics systems at LBT: FLAO commissioning and science operations status," in [*Adaptive Optics Systems III*], *Proc. SPIE* **8447**, 84470U (2012).

[8] Stockton, A., Canalizo, G., Nelan, E. P., and Ridgway, S. E., "Two Active Nuclei in 3C 294," *Astrophysical Journal* **600**, 626–633 (2004).

[9] Quirrenbach, A., Roberts, J. E., Fidkowski, K., de Vries, W., and van Breugel, W., "Keck Adaptive Optics Observations of the Radio Galaxy 3C 294: A Merging System at z=1.786?," *Astrophysical Journal* **556**, 108–112 (2001).

[10] Oya, S., Minowa, Y., Terada, H., Watanabe, M., Hattori, M., Hayano, Y., Saito, Y., Ito, M., Pyo, T.-S., Takami, H., and Iye, M., "Spatially Resolved Near-Infrared Imaging of a Gravitationally Lensed Quasar, APM 08279+5255, with Adaptive Optics on the Subaru Telescope," *Publ. Astron. Soc. Japan* **65**, 9 (2013).